1993ApJ...419..485M

THE ASTROPHYSICAL JOURNAL, 419:485–493, 1993 December 20
© 1993. The American Astronomical Society. All rights reserved. Printed in U.S.A.

CHEMICAL EVOLUTION OF GALAXIES AND QUASAR METALLICITIES

FRANCESCA MATTEUCCI[1] AND PAOLO PADOVANI[2]
Received 1993 April 20; accepted 1993 June 29

ABSTRACT

As part of a continuing investigation of the connection between observational properties of active galactic nuclei and their host galaxies, we study the evolution of the chemical composition of the gas lost by stars in elliptical galaxies and bulges of spirals by means of a self-consistent model of galactic evolution. It is found that with Salpeter-like, or flatter, initial mass functions, solar abundances are reached in a few 10^8 yr, thereby explaining in a natural way the standard emission lines observed in high-redshift quasars. Furthermore, after the first Gyr, the same mass functions give rise to overabundances of N, Si, and Fe, and roughly solar abundances of C, Ne, O, and Mg, only weakly time-dependent. These results are consistent with the (few) available abundance estimates for the gas emitting the broad lines observed in quasar spectra and, in particular, they could solve the puzzle of the quasi-similarity of quasar spectra at different redshifts. Finally, the metal overabundances inferred in high-redshift quasars are inconsistent with the association of these objects with newly formed galaxies as prescribed, for example, by the starburst model of active galactic nuclei, since in this case quasars should have abundance ratios very different from the estimated ones as well as lower absolute abundances. A criterion for distinguishing between the early burst and other hypothesis is given on the basis of the predicted abundance ratios.

Subject headings: galaxies: abundances — galaxies: elliptical and lenticular, cD — galaxies: evolution — quasars: general

1. INTRODUCTION

One of the (many) puzzling features of active galactic nuclei (AGNs) is the apparent similarity, at first order, of the spectra in different objects and at different redshifts: see, e.g., Véron-Cetty, Véron, & Tarenghi (1983) and compare, for example, the composite quasar spectrum published by Francis et al. (1991) with the spectra of high-redshift ($z \gtrsim 4$) quasars studied by Schneider, Schmidt, & Gunn (1991). Although deriving elemental abundances from emission lines requires a detailed model of the spectra (that is, the relationship between line ratios and metallicity depends, among other factors, on the ionization parameter, the electron density, and the shape of the ionizing continuum; see, e.g., Hamann & Ferland 1992, 1993a, b), this similarity could be taken to suggest similar metal abundances and in particular a negligible redshift dependence of quasar metallicities. It is in any case very interesting that high-redshift quasars, in particular, display "standard" emission lines like O VI 1034 Å, N V 1240 Å, and C IV 1550 Å, which shows that metal production was well underway in these young ($t \lesssim 2$ Gyr; $H_0 = 50$ km s^{-1} Mpc^{-1}, $q_0 \geq 0.1$) AGNs.

In a previous paper (Padovani & Matteucci 1993, hereafter Paper I), we have studied the connection between some observational features of AGNs and their host galaxies using a self-consistent model of galactic evolution which reproduces the main features of elliptical galaxies. In particular, we explored the relationship between stellar mass loss and the fueling of the central nucleus.

The purpose of this paper is to use the galactic evolution model employed in Paper I to follow in great detail the evolution of several chemical species, namely C, N, O, Ne, Mg, Si, and Fe, by taking into account detailed nucleosynthesis from stars of all masses and supernovae (SNs) of all types. Under the assumption that quasar broadlines are emitted by gas well mixed with the galactic interstellar medium (ISM), the chemical evolution in galaxies can be used to predict quasar metal abundances and their redshift dependence and these predictions can in turn be compared with the (few) abundance estimates available.

During the completion of this work, we received a preprint by Hamann & Ferland (1993a) in which these authors study similar problems. We want to stress that our approach is different from theirs, since no self-consistent treatment of the development of a galactic wind (see § 2) is included in their model (this applies also to Hamann & Ferland 1992). Some of the nucleosynthesis prescriptions are also different (see § 2), while the supernova progenitors are similar to those adopted here. In § 2 we describe the galactic evolution model adopted in this paper, while § 3 describes our results, discussed in § 4. Finally, § 5 presents our conclusions. Throughout this paper we use the standard notation [element/H] $\equiv$ log (element/H) − log (element/H)$_\odot$ and a value $H_0 = 50$ km s^{-1} Mpc^{-1}.

2. THE GALACTIC EVOLUTION MODEL

The adopted model of galactic evolution, which belongs to the category of supernova (SN) driven galactic wind models, is the one given in Paper I, Matteucci (1992), Brocato et al. (1990), Matteucci & Tornambè (1987), where a full description can be found. Here we summarize the main points.

The model, which is thought to describe an elliptical galaxy, is a one-zone model and assumes instantaneous mixing of gas. The assumed age for all galaxy models is $t_G = 15$ Gyr. The volume gas density in the form of a given element is derived at each time by solving an equation which takes into account depletion of the elements by star formation (assumed to drop to zero at the onset of a galactic wind) and restoration to the

[1] European Southern Observatory, Karl-Schwarzschild-Strasse 2, D-8046 Garching bei München, Germany.
Internet: fmatteuc@eso.org
[2] Astrofisica, Dip. di Fisica, II Università di Roma "Tor Vergata," Via della Ricerca Scientifica 1, I-00133 Roma, Italy.
Internet: padovani@roma2.infn.it

© American Astronomical Society • Provided by the NASA Astrophysics Data System

1993ApJ...419..485M

ISM by stellar mass loss due both to stellar winds and SN explosions. The initial mass function (IMF) is assumed to be constant in space and time and expressed as a power law with index x. The normalization of the IMF is performed by assuming a stellar mass range of 0.1–100 $M_\odot$, unless otherwise indicated.

The star-formation rate is assumed to be linearly proportional to the volume gas density. The proportionality constant, that is the efficiency of star formation (namely the star-formation rate per unit mass) expressed in units of Gyr^{-1}, as well as the adopted stellar lifetimes, are given in the above mentioned papers. Type Ia SNs are assumed to originate from white dwarfs in binary systems according to the model of Whelan & Iben (1973). The computation of the Type Ia SN rate follows the prescriptions given in Greggio & Renzini (1983a) and Matteucci & Greggio (1986). The nucleosynthesis prescriptions for Type II SNs (e.g., stars with $M > 10\ M_\odot$) are taken from Woosley (1987) and Arnett (1991), those for Type Ia SNs are from Nomoto, Thielemann & Yokoi (1984) (their model W7) and those for single intermediate mass stars ($0.8 \leq M/M_\odot \leq 8$) are from Renzini & Voli (1981). In particular, we adopted their case $\alpha = 0$ and $\eta = 0.33$. The case with $\alpha = 0$ does not predict any primary production of N and ^{13}C, so that these elements are produced in a purely secondary way. Generally, a chemical element is considered "secondary" from the nucleosynthetic point of view when it is produced proportionally to the initial metal content of the star. Typical in this respect is the production of N and ^{13}C as by-products of the CNO cycle. On the other hand, a "primary" element is produced from the original H and He content, independently of the initial stellar metallicity. For values of $\alpha > 0$ Renzini & Voli (1981) predicted that some primary N and ^{13}C were produced as a result of the hot-bottom burning acting in conjunction with the third dredge-up in massive asymptotic giant branch (AGB) stars. In fact, N and ^{13}C produced during the burning at the bottom of the convective envelope derive from C and O produced by the star itself, which are dredged up by convection, and therefore they have a primary nature. We chose the case with $\alpha = 0$ for two reasons; one is because with this choice of α we reproduce at best the abundances of C and N in the solar neighborhood (see D'Antona & Matteucci 1991). The second reason is that Blöcker & Schönberner (1991) have shown that the third dredge-up in massive AGB stars, with efficient hot-bottom burning, should not occur. This result, beside providing a natural explanation for the long-standing problem of the overproduction of bright AGB stars by synthetic AGB models, as discussed by Renzini (1993), suggests that the primary production of N and ^{13}C in intermediate mass stars should be almost suppressed. Therefore, it is somewhat justified to ignore the primary N and C production.

No overshooting is taken into account in the adopted yields. In a recent paper studying the chemical evolution of quasars Hamann & Ferland (1992) adopted N yields which are higher than those adopted here. These authors, in fact, summed the N yields given by Renzini & Voli (1981) with those of Talbot & Arnett (1973) for low- and intermediate-mass stars, claiming that doing so they were reproducing the yields (without overshooting) given by Serrano (1986). We do not agree with this choice since it overproduces N in the solar neighborhood when the model of Matteucci & François (1989) is adopted. In fact, although our prescriptions for N production in massive stars (Talbot & Arnett 1973, their case B) predict a higher amount of N than that assumed by Hamann and Ferland, the bulk of N is always produced in low- and intermediate-mass stars.

The existence of galactic winds in ellipticals was first suggested by Mathews & Baker (1971) and then by Larson (1974) in order to reproduce the well-known mass-metallicity relation and also to explain the apparent lack of gas in these systems. Although we now know, from X-ray studies of ellipticals, that these systems contain a substantial fraction of hot gas (10^8–$10^{11}\ M_\odot$; e.g., Fabbiano 1989), still the existence of a wind phase at some stage of evolution of these galaxies is required both to avoid overproducing gas and to explain the observed iron abundance in the intracluster medium (Matteucci & Vettolani 1988; Ciotti et al. 1991; Arnaud et al. 1992). For gas to be expelled from a galaxy the thermal energy of the gas heated by SN explosions should exceed its binding energy (Larson 1974). At this point the gas present in the galaxy is swept away. After the wind has occurred the gas restored by the dying stars is likely to be hot, as Type Ia SNs continue to inject energy in the rarified ISM (which is probably responsible for the observed X-ray emission in ellipticals). It is then justified to assume that no star formation will take place after the galactic wind and that the subsequent evolution is determined only by the amount of matter and energy which is restored to the ISM by the dying stellar generations. In particular, only low-mass stars contribute to this evolutionary phase and, among the SNs, only SNs of Type Ia which are those with the longest lifetimes. Again we refer the reader to the above mentioned papers for a detailed explanation of the calculation of the thermal energy content of the ISM, as due to the energy deposited by SNs, and the potential energy of gas. Massive but diffuse halos of dark matter are taken into account in the way described in Paper I. The initial luminous masses considered here are 10^{11}, 10^{12}, and $5 \times 10^{12}\ M_\odot$. This mass range corresponds to present-day ellipticals with luminosities in the range 5×10^9–$3 \times 10^{11}\ L_{B\odot}$ (Brocato et al. 1990), consistent with the results of Smith et al. (1986) on quasar host galaxies.

In order to compute the chemical evolution of the Galactic bulge we used the model for ellipticals with an initial mass of $10^{10}\ M_\odot$ and an efficiency of star formation of 15 Gyr^{-1}. The IMF adopted for the bulge has a slope $x = 1.1$, as suggested by Matteucci & Brocato (1990) in order to reproduce the observed distribution of bulge stars with metallicity. However, in order to reproduce such a distribution one needs to assume that star formation in the bulge lasted longer than expected from our standard models for ellipticals: in particular, if star formation was active for at least 1 Gyr, the metallicity distribution of bulge stars is very well fitted. A model for an elliptical galaxy with initial luminous mass of $10^{10}\ M_\odot$ would in fact develop a galactic wind very soon (after few 10^8 years) and the resulting stellar metallicity distribution would not fit the observed one (Rich 1988; Geisler & Friel 1992). The assumption of no galactic wind (or late wind) for the bulge is justified by the fact that the bulge does not evolve like an isolated elliptical galaxy of the same mass, since it lies at the bottom of a much deeper potential well defined by the rest of the Galaxy.

The chemical evolution of the solar neighborhood, which is used as a comparison, is performed by means of the model described in Matteucci & François (1989). This model is able to reproduce most of the observational constraints relative to the solar neighborhood and the whole disk. The nucleosynthesis prescriptions are common to all of these models. The main differences between the elliptical models and the solar neighborhood model are the efficiency of star formation which

© American Astronomical Society • Provided by the NASA Astrophysics Data System

1993ApJ...419..485M

goes from 15 to 7.15 Gyr^{-1} for ellipticals and is only 0.5 Gyr^{-1} in the solar neighborhood, and the IMF. In particular, for the solar neighborhood we used the IMF suggested by Scalo (1986) with a slope $x = 1.7$ in the range of massive stars, whereas the models for ellipticals and the Galactic bulge require flatter slopes. Finally, the disk models do not include the development of a galactic wind.

3. RESULTS

The time dependencies of the abundances of the elements under study are shown in Figure 1 for our standard galaxy of 10^{12} $M_\odot$ and a Salpeter ($x = 1.35$) IMF. Note the fast increase in the abundances at early times and the relatively weak decrease at later times: for $t \gtrsim 1$ Gyr, which corresponds to $z \lesssim 4.5$–7.8 for q_0 in the range 0.5–0.1, all abundances decrease at maximum by a factor of 2.5 over a period of 14 Gyr (the derived redshifts assume that star formation starts at the big bang; however, even if star formation starts up to 0.3 Gyr later, the redshift dependence for $z \lesssim 5$ will change very little for $q_0 = 0.5$ and even less for smaller values of q_0). It is also interesting to note that after the first Gyr the elements divide into two classes: the ones with roughly (within a factor of 2–3) solar abundances (C, Ne, O, and Mg) and the ones with abundances in the range 5–10 times solar (N, Si, and Fe). The mean ($t \gtrsim 1$ Gyr) metallicity is about three times solar. Table 1 gives the mean abundances and metallicities for $t \geq 1$ Gyr for various models.

Those elements showing roughly solar abundances for most of the galactic lifetime are the so-called α-elements (O, Ne, Mg). They are mainly produced in massive stars ($M > 10$ $M_\odot$) on short timescales of the order of 10^6 to several 10^7 years at maximum, reaching quite soon a sort of saturation value. In addition, their abundances cannot increase any more after the occurrence of the galactic wind ($t \simeq 1.4$ Gyr for this model) since star formation is no more active. Actually, they tend to decrease due to the dilution effect of stellar mass loss. Carbon is also behaving like the α-elements, although it is substantially produced in low- and intermediate-mass stars. This is due to the fact that C is used up by stars to form N, especially in low and intermediate mass stars where the bulk of N originates. Silicon behaves differently from the other α-elements since it is in part produced by Type Ia SNs on very long timescales. Also, elements such as N and Fe, which are mostly produced by low- and intermediate-mass stars, are restored to the ISM on timescales going from several 10^7 years to a Hubble time. Therefore, their abundances can in principle continue to increase even after star formation has stopped.

The effect of the IMF slope on abundances is shown in Figures 2 and 3 for x equal to 0.95 and 2, respectively. As shown in Paper I, the range of slopes cannot be much larger since both flatter ($x \lesssim 0.8$) and steeper ($x \gtrsim 2.2$) IMFs would give too large M/L ratios.

In the $x = 0.95$ case (Fig. 2), the larger proportion of massive stars implies higher abundances at early times, when star formation is more active. Fe and Si reach higher peak values at $t \sim 2$ Gyr, but their decrease is faster so that at $t \simeq 15$ Gyr their abundances are slightly less than for a Salpeter IMF. Overall, the mean abundances at $t \gtrsim 1$ Gyr are within 50% from the Salpeter values (see Table 1), while the abundance decrease at $t \gtrsim 2$ Gyr is of a factor of 5 for Fe and Si and at maximum of a factor of 2 for the other elements. The mean ($t \gtrsim 1$ Gyr) metallicity is still about 3 times solar. The $x = 2$ case (Fig. 3) represents a very steep IMF with a much smaller number of massive and intermediate mass stars. It then follows that all abundances are less than for a Salpeter IMF and, in

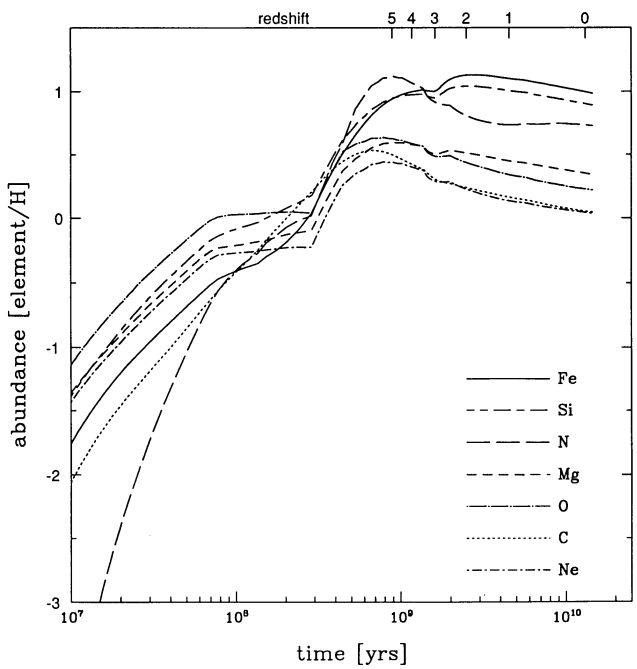

FIG. 1.—Time-dependence of the abundances of various elements relative to solar for a galaxy with a luminous mass of 10^{12} $M_\odot$ and a Salpeter ($x = 1.35$) IMF. Standard notation is used, i.e., $[Fe/H] \equiv \log (Fe/H) - \log (Fe/H)_\odot$. The different curves denote different elements as indicated in the lower right corner. The scale on the top axis gives the redshift corresponding to different times for $H_0 = 50$ km s^{-1} Mpc^{-1} and $q_0 = 0.5$. The discontinuity at $t \sim 0.3$ Gyr is due to the maximum in the Type Ia SN rate, which occurs at that epoch.

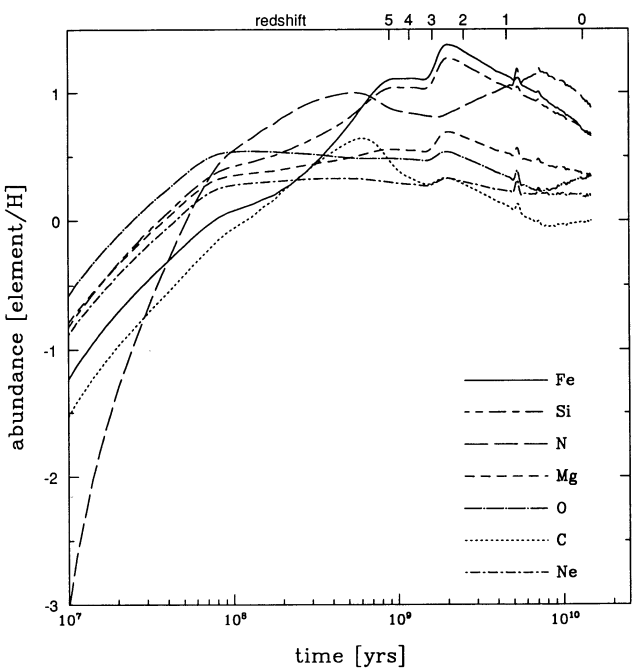

FIG. 2.—Time-dependence of the abundances of various elements relative to solar for a galaxy with a luminous mass of 10^{12} $M_\odot$ and an IMF slope $x = 0.95$. Standard notation is used, i.e., $[Fe/H] \equiv \log (Fe/H) - \log (Fe/H)_\odot$. The different curves denote different elements as indicated in the lower right corner. The scale on the top of axis gives the redshift corresponding to different times for $H_0 = 50$ km s^{-1} Mpc^{-1} and $q_0 = 0.5$.

© American Astronomical Society • Provided by the NASA Astrophysics Data System

1993ApJ...419..485M

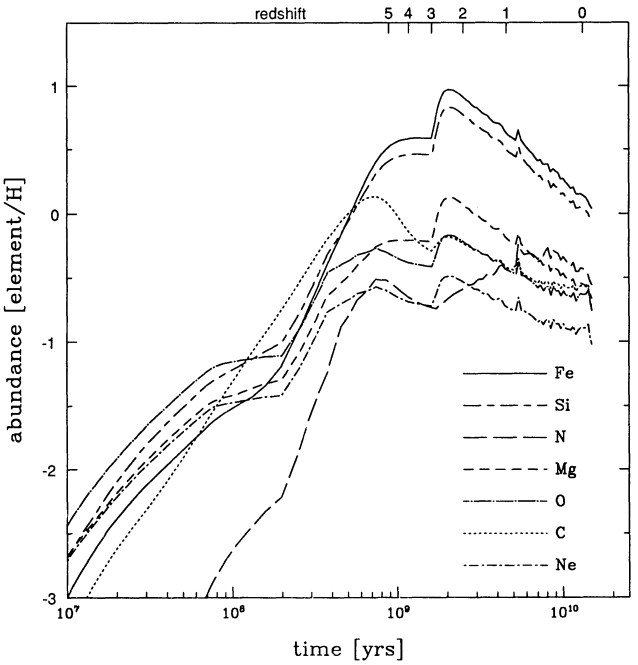

FIG. 3.—Time-dependence of the abundances of various elements relative to solar for a galaxy with a luminous mass of $10^{12}\ M_\odot$ and an IMF slope $x = 2.0$. Standard notation is used, i.e., $[Fe/H] \equiv \log (Fe/H) - \log (Fe/H)_\odot$. The different curves denote different elements as indicated in the lower right corner. The scale on the top axis gives the redshift corresponding to different times for $H_0 = 50$ km s^{-1} Mpc^{-1} and $q_0 = 0.5$. The discontinuity at $t \sim 0.3$ Gyr is due to the maximum in the Type Ia SN rate, which occurs at that epoch.

particular, at $t \simeq 15$ Gyr only Fe and Si are at solar levels while all other elements have abundances of the order of $\frac{1}{5}$ solar. The mean ($t \gtrsim 1$ Gyr) metallicity is in this case about 60% the solar one, a decrease of a factor of 5 from the two previous cases. The most important effect producing the decrease of element abundances at later times in the case $x = 0.95$ is the fact that the galaxy is in a steady-wind phase since the beginning of the galactic wind. The wind, which is treated as a series of instantaneous events where each time all of the ISM is expelled, is then subtracting metals from the gas. This effect coupled with stellar ejecta containing mostly hydrogen produces the abundance decrease. On the other hand in the Salpeter case, after the early wind (which lasts a few 10^8 years) has occurred, the energy restored to the ISM by SNs is not enough to trigger another wind and therefore the gas restored by dying stars remains bound to the parent galaxy. The occurrence of a steady wind is due to the delicate balance between the thermal and potential energy of the gas, and such a balance is very sensitive to the assumed IMF which changes the supernova rates and the occurrence of the first wind. In particular, in the $x = 0.95$ case the SN rates are higher so the wind occurs earlier than in the Salpeter case. The number of the more massive Type Ia SNs is also increased so that the energy input to the ISM is high enough to sustain a steady wind. In fact, if the SN energy after the first wind is high enough, the process can easily become continuous, since the wind devoids more and more the galaxy of gas decreasing in that way the potential energy. In the $x = 2.0$ case, the galactic wind occurs later than in the Salpeter case because of the lower Type II SN rate. A continuous wind is not established in this case and the decrease of the abundances at late times is due to the dilution effect by stellar mass loss, which is higher than in the other cases because of the larger number of low-mass stars.

To study the abundances in the nuclei of spirals, we show in Figure 4 the results for the bulge of our Galaxy. Given the somewhat flatter IMF ($x = 1.1$), the higher abundances (as compared with a Salpeter IMF) at early times are expected, while at later times ($\gtrsim 1$ Gyr) the results are not very different from a Salpeter or even a flatter IMF. No Galactic wind is assumed to occur in the bulge, as already mentioned before, and star formation is assumed to stop at around 1 Gyr, as due to the low gas density. In this situation the gas restored by stars remains bound to the Galaxy and it is only slightly affected by the stellar mass loss.

Figure 5 shows the abundance versus age relation for the elements under study for the solar neighborhood. The difference with previous models is striking. This is due to the much slower evolutionary rate assumed, which translates into a much less efficient star formation and a much longer collapse timescale as compared to elliptical galaxies: as a consequence, the predicted increase of the abundances with time is much slower. The abundances are of course all solar at the time of formation of the solar system ($t \simeq 8.5$ Gyr, where the present age of the disk is 13 Gyr).

Elliptical galaxies obey the well known mass (luminosity)-metallicity relationship, that is the average metallicity of the stars dominating the visual light increases with galactic mass (and luminosity) (Vader 1986). It is interesting then to see if a similar relationship exists between the metallicity of the gas and the mass of the galaxy. Figure 6 shows the mean values of the abundances for $t \geq 1$ Gyr, a Salpeter IMF, and a range of three different masses: 10^{11}, 10^{12}, and $5 \times 10^{12}\ M_\odot$. It can be seen that the abundances increase going from a 10^{11} to a 10^{12} $M_\odot$ galaxy, but then the relationship flattens, probably due to a dilution effect (i.e., the metal abundances decrease due to the higher fraction of H-rich gas restored by low-mass stars) which

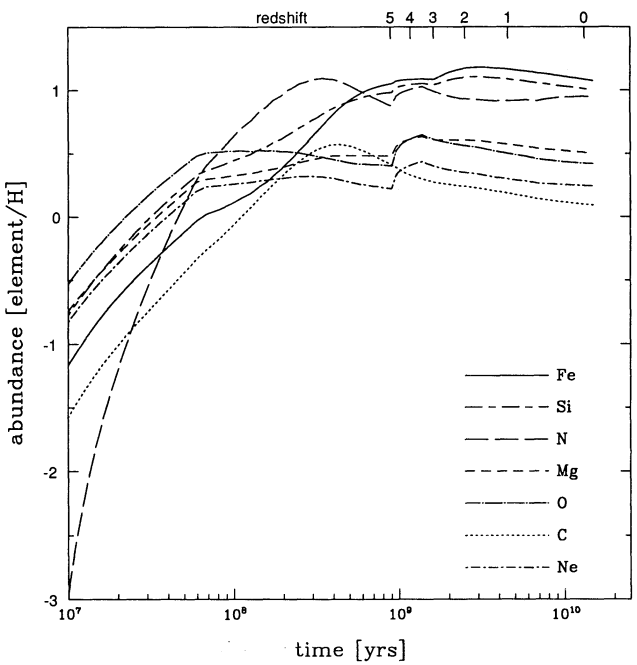

FIG. 4.—Time-dependence of the abundances of various elements relative to solar for the bulge of the Galaxy (mass of $10^{10}\ M_\odot$ and IMF slope $x = 1.1$). Standard notation is used, i.e., $[Fe/H] \equiv \log (Fe/H) - \log (Fe/H)_\odot$. The different curves denote different elements as indicated in the lower right corner. The scale on the top axis gives the redshift corresponding to different times for $H_0 = 50$ km s^{-1} Mpc^{-1} and $q_0 = 0.5$.

© American Astronomical Society • Provided by the NASA Astrophysics Data System

1993ApJ...419..485M

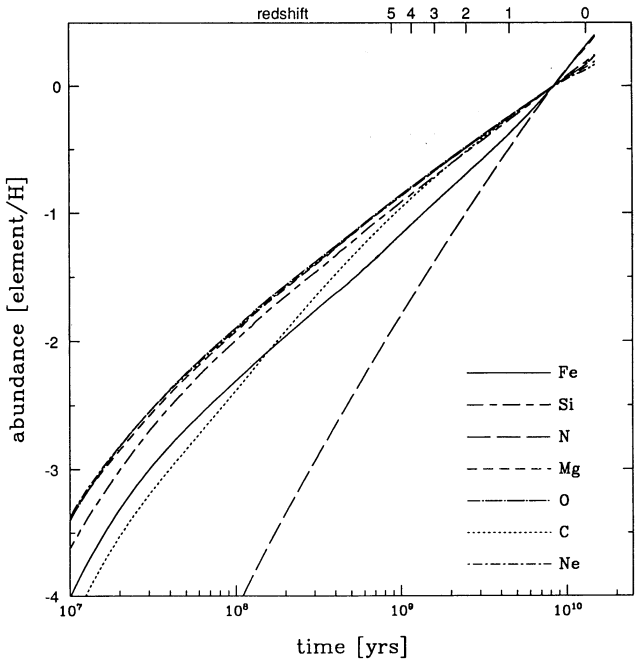

FIG. 5.—Time-dependence of the abundances of various elements relative to solar for the solar neighborhood model of Matteucci & Francois (1989). Standard notation is used, i.e., $[Fe/H] \equiv \log (Fe/H) - \log (Fe/H)_\odot$. The different curves denote different elements as indicated in the lower right corner. The scale on the top axis gives the redshift corresponding to different times for $H_0 = 50$ km s^{-1} Mpc^{-1} and $q_0 = 0.5$.

is relatively more efficient at higher masses. Note that the shape of the metallicity-mass relationship is similar for O, Ne, Mg, Si, and Fe, which implies that abundance ratios involving these elements are basically independent of the mass of the galaxy. They in fact depend mostly on the assumed IMF. The situation is different for C and N since N, being a "secondary" element, depends very strongly on the galaxy metallicity (mass) and it is formed at the expense of C. As a consequence of this N increases with galactic mass while C decreases slightly. This implies that abundance ratios involving these elements will depend on the mass of the galaxy and, in particular, that [N/C] will be larger in more massive galaxies.

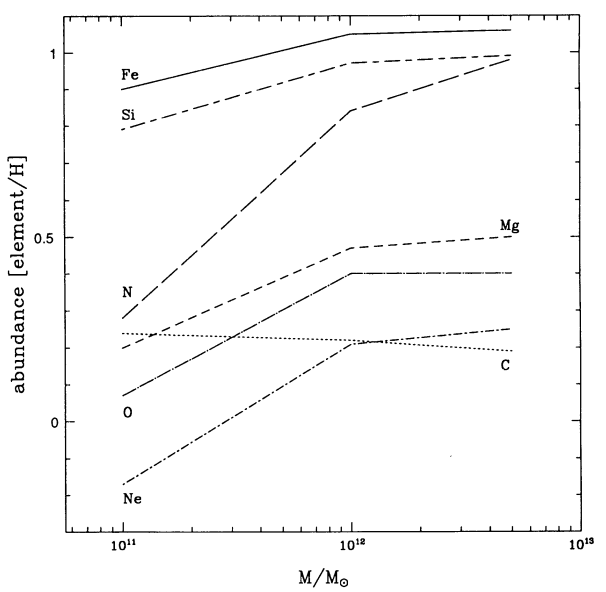

FIG. 6.—Dependence of the mean abundances (for $t \geq 1$ Gyr) of various elements relative to solar on galaxy mass for a Salpeter ($x = 1.35$) IMF. Standard notation is used, i.e., $[Fe/H] \equiv \log (Fe/H) - \log (Fe/H)_\odot$. The different curves denote different elements as indicated.

4. DISCUSSION

In this section we would like to compare our predictions with the abundances inferred in the broad line regions (BLRs) of AGNs. We stress that we will not try to reproduce the (scanty) observational data on quasar metallicities by changing the parameters of the model, since these have already been constrained by the main observational features of elliptical galaxies, such as stellar metal content, luminosity, M/L ratios, current SN rates (e.g., Matteucci 1992; Brocato et al. 1990). It is also important to keep in mind that, as mentioned in § 1, elemental abundances derived from quasar emission lines are model-dependent, since the results can vary with the assumed ionizing continuum, electron density, and ionization parameter (e.g., Hamann & Ferland 1992, 1993a, b).

4.1. *Inferred Quasar Abundances*

Photoionization models usually *assume* solar abundances or only slight overabundances (see, e.g., the review by Collin-Souffrin & Lasota 1988). Detailed comparisons with observed line ratios, however, seem to suggest significant overabundances of some elements. In particular:

1. Kallman et al. (1993) could not reproduce the observed line ratios in a C IV/Lyα versus N V/Lyα plot for 12 quasars with $z \simeq 2$ unless (N/C) were about 7 times the solar value. Hamann & Ferland (1992) have shown that N V/C IV line ratios suggest an (N/C) overabundance ranging between 2 and 10 times solar in a large number of high-redshift ($z \gtrsim 2$) quasars. Uomoto (1984) has derived an average (N/C) which is about twice solar for six quasars with $z \simeq 2$, while (O/C) was basically solar. Note that nitrogen overabundance has also been inferred in the nuclei of Seyfert 2 (Storchi-Bergmann & Pastoriza 1989) and spiral (e.g., Alloin 1973) galaxies.

2. The existence of an "Fe II problem" in the BLR was stressed by Wills, Netzer, & Wills (1985) and by Collin-Souffrin et al. (1986). Namely, standard photoionization models predict Fe II to hydrogen-line (and also Fe II to Mg II) ratios about a factor of 3 smaller than the average observed ones, reaching in some individual cases factors of 10. One way out of the problem would be an iron overabundance of about an order of magnitude as compared to solar values (e.g., Collin-Souffrin & Lasota 1988).

3. Studying the relative contribution of Si IV λ1397 and O IV] λ1402 to the λ1400 feature in quasar spectra, Wills & Netzer (1979) noticed that if O IV] were the dominant contributor, as suggested by their analysis of the mean rest wavelength of the feature, one would either have inferred oxygen abundances at odds with those derived from other oxygen lines, or one would have needed a collisional cross section of O IV] larger by a factor of 3 than the (quite uncertain) one available at the time. However, a subsequent detailed calculation by Hayes (1982) confirmed the value of the collisional cross section adopted by Wills & Netzer (1979). Recent determinations of the mean rest wavelength of the feature, based on higher quality data (e.g., Tytler & Fan 1992, and references therein), however indicate an average ratio of Si IV λ1397 to

© American Astronomical Society • Provided by the NASA Astrophysics Data System

1993ApJ...419..485M

O IV] λ1402 near, or larger than, unity. In that case (Si/N) and (Si/O) would be larger than solar (Wills & Netzer 1979).

The main conclusion seems to be that BLR line ratios suggest N, Fe, and possibly Si overabundances (up to a factor of 10, at least for the first two elements), while for other elements there seems to be no evidence for abundances much different from solar. At present no detailed photoionization studies have looked for possible redshift dependencies of BLR abundances but the approximate similarity of quasar spectra at different redshifts (discussed in § 1) seems to rule out at least order-of-magnitude changes.

The inferred overabundances would then be consistent with Salpeter-like ($x = 1.35$) or even flatter ($x = 0.95$) IMFs, but they seem to rule out steep IMFs (see Figs. 1–3 and Table 1). In this latter case in fact, for $t \gtrsim 1$ Gyr most elements are between 10 and 50% solar, with only Fe and Si between 2 and 3 times solar, while N is underabundant at all times. The predicted time dependence of the abundances range from very weak ($x = 1.35$) to strong ($x = 2$) and again the observational data might favor flatter slopes, since the $x = 2$ case, for example, predicts an order of magnitude decrease in the Fe and Si abundances for $t \gtrsim 2$ Gyr ($z \lesssim 2.5$ or 4.2 for $q_0 = 0.5$ or 0.1, respectively). These predictions apply to elliptical galaxies and therefore, given the observational evidence that the image profiles of the host galaxies of radio-loud quasars are better represented by elliptical models (e.g., Smith et al. 1986; Hutchings, Janson, & Neff 1989), these results should refer only to radio-loud quasars. The situation for the more numerous radio-quiet quasars, which are thought to reside in spiral galaxies, is however not very different. Figure 4 and Table 1 show that bulges of spirals are predicted to have N, Si, and Fe overabundances and a weak time dependence for all abundances at $t \gtrsim 0.1$–1 Gyr, again a situation consistent with the observational data.

A more direct source of information on chemical abundances in the gas of elliptical galaxies is provided by X-ray spectroscopy of NGC 1399 and NGC 4472 recently obtained with the *Broad Band X-ray Telescope* (BBXRT) (Serlemitsos et al. 1993). At variance with what is inferred from BLRs in AGNs, these observations seem to indicate that the iron abundance in the hot gas of these ellipticals is subsolar. This fact would imply a minor role of Type Ia SNs in the chemical enrichment of elliptical galaxies. However, one of the main assumptions used to derive such abundances is that the abundance ratios are solar. This is in contradiction with what is predicted by our model which assumes that the bulk of iron is indeed produced by Type Ia SNs. This assumption is also of fundamental importance in order to reproduce the behavior of several abundance ratios observed in solar neighborhood stars (Greggio & Renzini 1983b; Matteucci & Greggio 1986; Matteucci & François 1992). Therefore, if the abundance ratios in the gas in ellipticals are not solar, the inferred iron abundances should be revised. Moreover, NGC 1399 is the central galaxy in the Fornax cluster, while NGC 4472 is the brightest galaxy in the Virgo cluster: dilution effects due to accretion of unenriched external gas could then play a role in determining the final abundances in the gas of these ellipticals. In summary, we feel that a direct comparison of the BBXRT results with our predicted abundances is still premature.

4.2. [N/C] *Ratios*

Further observational constraints can be given by the [N/C] ratios derived by Hamann & Ferland (1992) from a detailed photoionization model and N V/C IV line ratios measured in a few dozen quasars spanning the ranges $0 \lesssim z \lesssim 0.6$ and $1.8 \lesssim z \lesssim 4.9$. The [N/C] redshift dependencies (for $q_0 = 0.5$) predicted by our model for ellipticals with different IMFs, the Galactic bulge, and the solar neighborhood are shown in Figure 7. Also shown are the regions of the [N/C]–redshift plane occupied by the objects studied by Hamann & Ferland (1992), where we have used their results for $Z = 2.5Z_\odot$, which is appropriate for our elliptical models with $x = 0.95$ and 1.35, and the Galactic bulge (see Table 1).

The main conclusion which can be drawn from Figure 7 is that the typical abundance ratios [N/C] $\simeq 0.6$ dex inferred in high-redshift quasars can be explained by "standard" elliptical galaxy models with a Salpeter ($x = 1.35$), or even flatter ($x = 0.95$) IMF, and the Galactic bulge model, while steeper IMFs or a chemical evolution similar to the one of the solar neighborhood seem ruled out (note that adopting solar metallicities, which are appropriate for these latter models, Figure 2 of Hamann & Ferland [1992] implies higher [N/C] values, increasing even more the discrepancy with the data). As regards the highest values of [N/C] we believe they can be explained by a combination of factors, such as observational errors which can be as large as a factor of 2 when N V is strongly blended with Lyα; simplifying assumptions in the photoionization models, like constant density (higher densities would give higher [N/C] ratios: Hamann & Ferland 1992). It seems however that the mean inferred values of [N/C] *decreases* at lower redshifts, while the predictions would suggest constant or even increasing values. We interpret this as a simple selection effect, where the high-redshift objects, more luminous than the low-redshift ones, are probably associated with larger galaxies, while at low-redshift more common objects, residing in smaller galaxies, are selected. This, plus the [N/C]–mass relationship discussed in the previous section, can explain the observed trend. Figure 8 shows in fact the [N/C] redshift dependencies (for $q_0 = 0.5$) predicted by our model for ellipticals with a Salpeter IMF but different masses, where the

TABLE 1

ABUNDANCES

Model (1)	[C/H] (2)	[N/H] (3)	[O/H] (4)	[Ne/H] (5)	[Mg/H] (6)	[Si/H] (7)	[Fe/H] (8)	$Z/Z_\odot$ (9)
$M_{\rm in,lum} = 10^{12}\,M_\odot, x = 1.35$	0.22	0.84	0.40	0.21	0.47	0.97	1.05	2.9
$M_{\rm in,lum} = 10^{12}\,M_\odot, x = 0.95$	0.05	1.02	0.33	0.22	0.46	0.90	0.96	2.7
$M_{\rm in,lum} = 10^{12}\,M_\odot, x = 2.0$	−0.42	−0.49	−0.46	−0.75	−0.27	0.39	0.51	0.6
$M_{\rm in,lum} = 10^{10}\,M_\odot, x = 1.1$ (Bulge)	0.22	0.96	0.53	0.33	0.57	1.05	1.11	3.5

NOTES.—Col. (1): Model parameters, i.e., luminous mass of the galaxy, in solar masses, and IMF slope. Cols. (2)–(8): mean abundances ($t \geq 1$ Gyr) relative to solar [e.g., $[{\rm C/H}] \equiv \log({\rm C/H}) - \log({\rm C/H})_\odot$]. Col. (9): mean metallicity ($t \geq 1$ Gyr) relative to solar.

© American Astronomical Society • Provided by the NASA Astrophysics Data System

1993ApJ...419..485M

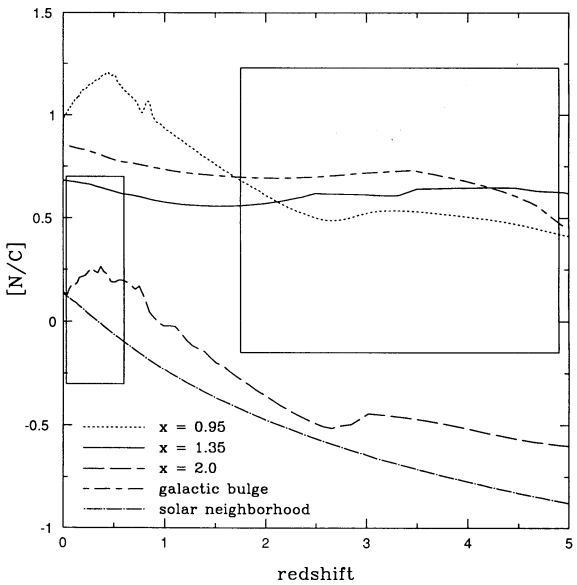

FIG. 7.—Redshift-dependence of the [N/C] ratio (for $H_0 = 50$ km s^{-1} Mpc^{-1} and $q_0 = 0.5$). The different curves denote different models and IMFs: an elliptical galaxy with a luminous mass of 10^{12} $M_\odot$ and $x = 1.35$ (*solid line*), $x = 0.95$ (*dotted line*), $x = 2.0$ (*long dashed line*); the Galactic bulge (*short dashed-long dashed line*); the solar neighborhood (*dotted-long dashed line*). Standard notation is used, i.e., $[N/C] \equiv \log (N/C) - \log (N/C)_\odot$. The two boxes show the range of [N/C] derived by Hamann & Ferland (1992) in two redshift intervals for $Z = 2.5Z_\odot$ (see test for additional details).

quite strong dependence of [N/C] on galactic mass, discussed in the previous section, is apparent. It can be seen that the typical [N/C] values inferred at low redshifts can be explained by a Salpeter IMF, as the high-redshift ones, and by lower galactic masses.

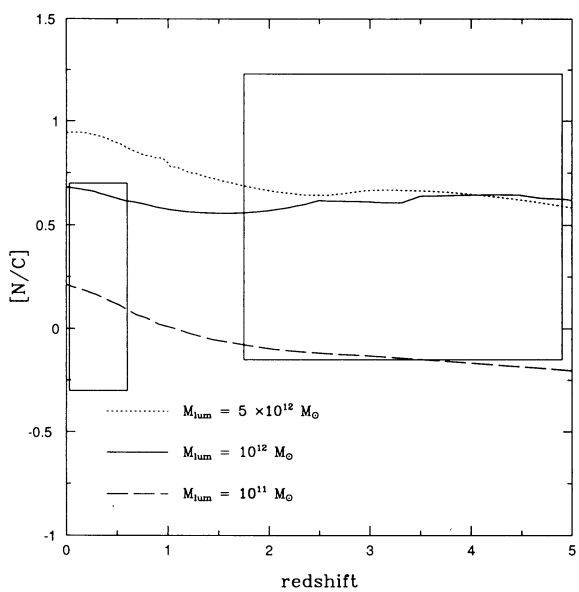

FIG. 8.—Redshift-dependence of the [N/C] ratio (for $H_0 = 50$ km s^{-1} Mpc^{-1} and $q_0 = 0.5$) for an elliptical galaxy with a Salpeter IMF ($x = 1.35$), and three different luminous masses: 10^{11} $M_\odot$ (*long-dashed line*), 10^{12} $M_\odot$ (*solid line*), and 5×10^{12} $M_\odot$ (*dotted line*). Standard notation is used, i.e., $[N/C] \equiv \log (N/C) - \log (N/C)_\odot$. The two boxes show the range of [N/C] derived by Hamann & Ferland (1992) in two redshifts intervals for $Z = 2.5Z_\odot$ (see text for additional details).

4.3. *Quasars as Nuclei of Young Galaxies?*

Our results are also very relevant to the so-called "starburst model" of AGNs, which states that the activity of these nuclei can be explained solely by young stars and supernova remnants, without the presence of a central black hole (e.g., Terlevich et al. 1992; Terlevich & Boyle 1993). In particular, if quasars are the young cores of massive ellipticals *forming* at $z \gtrsim 2$ and the quasar phase lasts from 8×10^6 up to $\sim 6 \times 10^7$ yr after the beginning of the burst, as suggested by Terlevich & Boyle (1993), Figures 1–4 show that their abundances should be well below solar for most elements (although absolute abundances are quite model-dependent). However, this argument applies to Terlevich and Boyle's hypothesis only if the quoted times for the beginning and end of the QSO phase are considered from the beginning of the star formation, in other words if the burst is the first and the main one: otherwise, the situation can be different, as discussed below.

A stronger constraint is provided by the gas abundance ratios which should be very different from those typical of older systems, irrespective of the assumed star-formation law. Figure 9 shows that a young elliptical has an [Fe/O] ratio of the order of -0.5 dex, independently of the particular model, i.e., about one order of magnitude smaller than an older ($t \gtrsim 1$ Gyr) one ([Fe/O] $\simeq +0.5$ dex). The same argument holds for the other α-elements and the reason for this behavior resides in the fact that in the early phases of star formation only SNs of Type II contribute to the gas enrichment. This is the same argument invoked to explain the trend of abundance ratios as a function of [Fe/H] observed in solar neighborhood stars (Greggio & Renzini 1983b; Matteucci & Greggio 1986; Matteucci & François 1992).

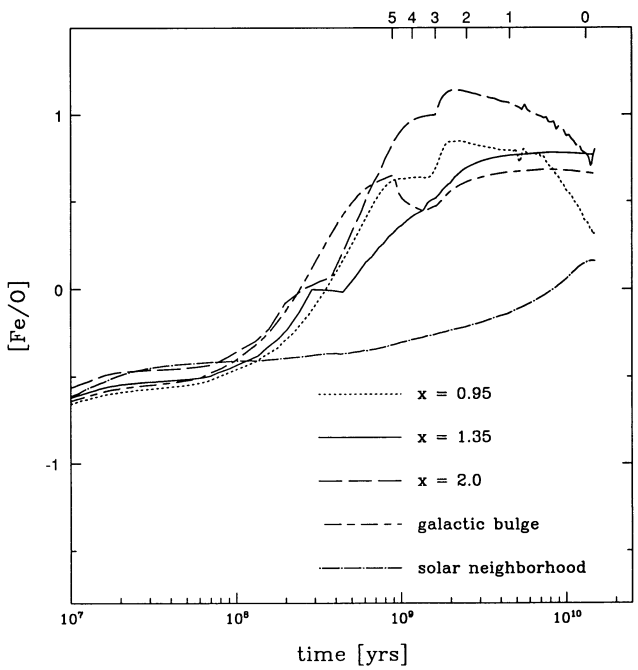

FIG. 9.—Time dependence of the [Fe/O] ratio relative to solar. The different curves denote different models and IMFs: an elliptical galaxy with a luminous mass of 10^{12} $M_\odot$ and $x = 1.35$ (*solid line*), $x = 0.95$ (*dotted line*), $x = 2.0$ (*long dashed line*); the Galactic bulge (*short dashed-long dashed line*); the solar neighborhood (*dotted-long dashed line*). Standard notation is used, i.e., $[Fe/O] \equiv \log (Fe/O) - \log (Fe/O)_\odot$. The scale on the top axis gives the redshift corresponding to different times for $H_0 = 50$ km s^{-1} Mpc^{-1} and $q_0 = 0.5$, assuming that star formation starts at the big bang.

© American Astronomical Society • Provided by the NASA Astrophysics Data System

1993ApJ...419..485M

The difference in the abundance ratios between early and late times can be even larger in the case of the (N/C) ratio which, for example, for a 2–3 $\times$ 10^7 yr old elliptical with a Salpeter IMF is about 1/10 solar, to be compared with 3 times solar for $t \gtrsim 1$ Gyr. The main point is that the (N/C) values inferred for high-redshift quasars are on average larger than solar (typically by a factor of 3 but in some cases possibly even up to a factor of 10), which is inconsistent with these objects being young cores of forming galaxies.

These results can be generalized to *any* model associating quasars with newly-formed galaxies, where by "formation" we mean the formation of the galaxy with its stars. For example, Haehnelt & Rees (1993), in the framework of the hierarchical scenario, have proposed that $z \gtrsim 0.5$ quasars constitute the first phase of the formation of a galaxy in the potential well of a dark matter halo. In this picture, quasars could "switch on" within a few 10^7 yr after the formation of the galaxy core and should therefore display abundances and abundance ratios [Fe/α] and [N/C] well below solar, at variance with observations.

It is important to notice that the effect of a "late" starburst, that is of a starburst episode superposed on the passive evolution of a galaxy which has already experienced the galactic wind, has only a small effect on the metal abundances. For example, our model shows that a starburst which lasts 10^8 yr at $t \simeq 10$ Gyr in the case of an elliptical galaxy with a luminous mass of 10^{12} $M_\odot$ and a Salpeter IMF, increases basically all abundances by only about a factor of 2, leaving almost unchanged the preexisting abundance ratios.

5. CONCLUSIONS

We have studied the time dependence of the chemical composition of the gas restored by stars to the interstellar medium in elliptical galaxies and bulges of spirals, by means of a self-consistent model of galactic evolution which has been shown to reproduce the main observational features of ellipticals. Assuming that the gas emitting the broad lines observed in quasar spectra is well mixed with the galactic interstellar medium, we have made specific predictions regarding quasar abundances of several chemical species, namely C, N, O, Ne, Mg, Si, and Fe, and their redshift dependence. In particular, our main results are the following:

1. Due to the high star-formation rate in ellipticals and bulges of spirals at early times, as compared to the solar neighborhood, solar abundances are reached in a few 10^8 yr after star formation starts for Salpeter-like, or flatter, IMF. This explains in a natural way the "standard" emission lines (e.g., O VI, N V, C IV) displayed by high-redshift ($z \gtrsim 4$) quasars.

2. After the first Gyr from the start of star formation ($z \lesssim$ 4.5–7.8 for $H_0 = 50$ and q_0 in the range 0.5–0.1) a Salpeter-like, or flatter, IMF predicts up to one order of magnitude overabundances for N, Si, and Fe, and roughly solar abundances for C, Ne, O, and Mg. This is not consistent with the few abundance estimates available for the broad-line regions of quasars. Moreover, the relatively weak time dependence predicted for the abundances at $t \gtrsim 1$ Gyr could explain the long-standing puzzle of the similarity of quasar spectra at different redshifts.

3. If quasars are associated with newly formed galaxies as predicted, for example, in the starburst model of AGN or in some quasar models based on the hierarchical growth of structure, they should have abundance ratios very different from those typical of older systems. A clear signature of an early starburst would in fact be ratios [Fe/α] and [N/C] $\lesssim 0$. These seem to be inconsistent with observations, in particular with the high values of [N/C] inferred in high-redshift quasars. The effect on the metal abundances of a late starburst, however, would be very small. These abundance ratios, therefore, can be used as a cosmic clock, as suggested also by Hamann & Ferland (1993a).

We acknowledge useful discussions with A. Cavaliere, A. Diaz, and R. Fosbury. We would like to thank the referee, F. Hamann, for his careful reading of the manuscript and useful suggestions.

REFERENCES

Alloin, D. 1973, A&A, 27, 433
Arnaud, M., Rothenflug, R., Boulade, L., Vigroux, L., & Vangioni-Flam, E. 1992, A&A, 254, 49
Arnett, D. W. 1991, in Frontiers of Stellar Evolution, ed. D. L. Lambert (ASP Conf. Ser., 20), 389
Blöcker, T., & Schönberner, D. 1991, A&A, 244, L43
Brocato, E., Matteucci, F., Mazzitelli, I., & Tornambè, A. 1990, ApJ, 349, 458
Ciotti, L., D'Ercole, A., Pellegrini, S., & Renzini, A. 1991, ApJ, 376, 380
Collin-Souffrin, S., Joly, M., Pequignot, D., & Dumont, S. 1986, A&A, 166, 27
Collin-Souffrin, S., & Lasota, J.-P. 1988, PASP, 100, 1041
D'Antona, F., & Matteucci, F. 1991, A&A, 248, 62
Fabbiano, G. 1989, ARA&A, 27, 87
Francis, P. J., Hewett, P. C., Foltz, C. B., & Chaffee, F. H. 1991, ApJ, 373, 465
Geisler, D., & Friel, E. D. 1992, AJ, 104, 128
Greggio, L., & Renzini, A. 1983a, A&A, 118, 217
———. 1983b, Mem. Soc. Astron. Ital., 54, 311
Haehnelt, M. G., & Rees, M. J. 1993, MNRAS, 263, 168
Hamann, F., & Ferland, G. 1992, ApJ, 391, L53
———. 1993a, ApJ, in press
———. 1993b, Rev. Mexicana Astron. Af., in press
Hayes, M. A. 1982, MNRAS, 199, 49P
Hutchings, J. B., Janson, T., & Neff, S. G. 1989, ApJ, 342, 660
Kallman, T. R., Wilkes, B. J., Krolik, J. H., & Green, R. 1993, ApJ, 403, 45
Larson, R. B. 1974, MNRAS, 169, 245
Mathews, W. G., & Baker, J. C. 1971, ApJ, 170, 241
Matteucci, F. 1992, ApJ, 397, 32
Matteucci, F., & Brocato, E. 1990, ApJ, 365, 539
Matteucci, F., & François, P. 1989, MNRAS, 239, 885
———. 1992, A&A, 262, L1
Matteucci, F., & Greggio, L. 1986, A&A, 154, 279
Matteucci, F., & Tornambè, A. 1987, A&A, 185, 51
Matteucci, F., & Vettolani, G. 1988, A&A, 202, 21
Nomoto, K., Thielemann, F. K., & Yokoi, K. 1984, ApJ, 286, 644
Padovani, P., & Matteucci, F. 1993, ApJ, 416, 26 (Paper I)
Renzini, A. 1993, in Galaxy Formation, ed. J. Silk & N. Vittorio (Varenna: SIF), in press
Renzini, A., & Voli, M. 1981, A&A, 94, 175
Rich, R. M. 1988, AJ, 95, 828
Scalo, J. M. 1986, Fund. Cosmic Phys., 11, 1
Schneider, D. P., Schmidt, M., & Gunn, J. E. 1991, AJ, 101, 2004
Serlemitsos, P. J., Loewenstein, M., Mushotzky, R. F., Marshall, F. E., & Petre, R. 1993, ApJ, 413, 518
Serrano, A. 1986, PASP, 98, 1066
Smith, E. P., Heckman, T. M., Bothun, G. D., Romanishin, W., & Balick, B. 1986, ApJ, 306, 64
Storchi-Bergmann, T., & Pastoriza, M. G. 1989, ApJ, 347, 195
Talbot, R. J., & Arnett, W. D. 1973, ApJ, 186, 51
Terlevich, R., & Boyle, B. J. 1993, MNRAS, 262, 491
Terlevich, R., Tenorio-Tagle, G., Franco, J., & Melnick, J. 1992, MNRAS, 255, 713
Tytler, D., & Fan, X.-M. 1992, ApJS, 79, 1
Uomoto, A. 1984, ApJ, 284, 497
Vader, P. 1986, ApJ, 305, 1669
Véron-Cetty, M.-P., Véron, P., & Tarenghi, M. 1983, A&A, 119, 69
Whelan, J., & Iben, I., Jr. 1973, ApJ, 186, 1007
Wills, D., & Netzer, H. 1979, ApJ, 233, 1
Wills, B. J., Netzer, H., & Wills, D. 1985, ApJ, 288, 94
Woosley, S. E. 1987, in Nucleosynthesis and Chemical Evolution, 16th Saas-Fee Course, ed. B. Hauck et al. (Geneva: Geneva Obs.), 1

© American Astronomical Society • Provided by the NASA Astrophysics Data System

1993ApJ...419..485M

Note added in proof.—R. Terlevich has pointed out to us that in his starburst model the core is metal-rich even before star formation starts there, because of the high-metallicity gas, produced by stars in the main body of the galaxy, falling into the central regions at the end of the galaxy formation phase, as predicted by classic dissipative models. In this case, if the bulk of the metal abundance in the gas falling in the core is produced before the starburst, our arguments regarding the age of the starburst based on abundance ratios do not apply. On the other hand, if the level of preenrichment in the gas is negligible relative to the enrichment produced by the starburst, then our arguments still apply. We note, in fact, that it is not at all clear from dissipative models of galaxy formation (R. B. Larson, MNRAS, 166, 585 [1974]) what is the amount of preenrichment predicted in the galactic nucleus before star formation *in situ* takes place. Moreover, in our opinion, it still needs to be proven that elliptical galaxies have formed from outside in and not from inside out.

© American Astronomical Society • Provided by the NASA Astrophysics Data System